

Graphene oxide modified H₄L-ion imprinting electrochemical sensor for the detection of uranyl ions

Yujie Li⁺,^[a] Zhimei Wang⁺,^[a] Chen Liu,^[b] Di Zhang,^[b] Lifu Liao,^[b] and Xilin Xiao^{*[a, b, c]}

The rapid development of the nuclear industry has gradually aroused people's attention to the problem of nuclear pollution. Due to the biological toxicity of uranium and its aqueous solution, simple and rapid detection of uranium in the water environment is quite important. An ion imprinted carbon nanomaterial (graphene oxide) electrochemical sensor for the detection of trace uranyl ions was prepared by using the synthesized bipolar tetradentate macrocyclic uranyl ligand cyclo-bis-phenylenediamine-bis-(phenylmethyl-diphyrrolecarbaldehyde) (H₄L) as functional monomer. The sol-gel polymer was prepared by hydrolysis and polymerization of H₄L ligand, 3-aminopropyltrimethoxysilane and tetraethoxysilane. H₄L-ion imprinted polymer (U-IIP) was prepared by adding 1 mM uranyl ion as template ions. Then the polymer was bonded to

graphene oxide modified carbon paste electrode, and the template ions were eluted to obtain H₄L-ion imprinted-graphene oxide modified carbon paste electrode (U-IIP/GO/CPE). Differential pulse voltammetry was used to detect trace uranyl ions. The results showed that the U-IIP/GO/CPE sensor system can detect uranyl ions with high sensitivity and specificity, and the peak current appeared around -0.26v. In the range of 0.01 μM ~ 3.0 μM, the detection current had a good linear relationship with the molar concentration of uranyl ions, and the method detection limit was 1.32 nM (S/N=3). Through the detection of actual samples, it had a good acceptable recovery rate (95.45% ~ 106.25%), and the relative standard deviation was less than 3.25%.

Introduction

Uranium is a radioactive and biotoxic metallic element that commonly causes environmental contamination through a variety of nuclear processes, including nuclear power generation, nuclear waste disposal, nuclear accidents,^[1] and the burning of fossil fuels.^[2] Humans may come into contact with uranium through inhalation of contaminated airborne dust or ingestion of contaminated food.^[3] While soluble uranium compounds can be excreted from the body to some extent, insoluble uranium compounds, especially in the form of dust, can be inhaled by the body and cause great harm when they adhere to the lungs.^[4] In addition, uranium that enters the body becomes uranyl ions (UO₂²⁺), which can accumulate and cause fatal damage to bones, liver, kidneys,

and reproductive tissues.^[5] Therefore, timely and accurate detection of trace amounts of uranium in the environment is essential for both healthy life and environmental protection.^[6] There are many methods for the detection of uranium, such as capillary zone electrophoresis,^[7] inductively coupled plasma emission spectroscopy,^[8] ion chromatography,^[9] inductively coupled plasma mass spectrometry,^[10] graphite furnace atomic absorption spectrometry,^[11] spectrophotometry,^[12] fluorescence^[13] and neutron activation analysis.^[14] Although these schemes offer the advantages of high sensitivity and low detection limits, they require expensive equipment as well as higher operating costs. In contrast, electrochemical sensors prepared using chemically modified electrodes are effective detection techniques that require low cost equipment, rapid analysis,^[15] ease of operation and high detection sensitivity.^[16] Moreover, among the conventional methods for the detection of uranyl ions in solution,^[17] adsorption solvation voltammetry (AdSV)^[18] is one of the most commonly used methods. When uranium forms complexes with surface active ligands and is deposited adsorptively on the electrode surface, it makes the sensitivity of the sensor further improved.^[19] Although suspended mercury droplets and mercury film electrodes have been used for AdSV determination of uranium, the biological toxicity of mercury has increased people's interest in non-mercury sensors.^[20] For this purpose, new electrode materials and methods for measurement of uranium have been developed, such as modified carbon paste electrodes,^[21] self-assembled monolayer gold-based electrodes,^[22] carbon nanotube modified electrodes,^[23] screen-printed electrodes,^[24] carbon fiber electrodes,^[25] and graphite electrodes.^[26]

Graphene, as a two-dimensional carbon nanomaterial, has received much attention due to its specific properties such as high surface area, excellent electrical conductivity and mechanical

[a] Y. Li,⁺ Z. Wang,⁺ Prof. Dr. X. Xiao

College of Resource & Environment and Safety Engineering,
University of South China,
Hengyang City 421001, P.R. China
E-mail: xiaoxl2001@163.com

[b] C. Liu, D. Zhang, Prof. L. Liao, Prof. Dr. X. Xiao

College of Chemistry and Chemical Engineering,
Hunan Province Key Laboratory of Typical Environmental
Pollution and Health Hazards,
University of South China,
Hengyang City 421001, P.R. China

[c] Prof. Dr. X. Xiao

State Key Laboratory of Chemo & Biosensing and Chemometrics,
Hunan University,
Changsha City 410082, Hunan Province, P.R. China

[⁺] Yujie Li and Zhimei Wang contributed equally to this work.

Supporting information for this article is available on the WWW under <https://doi.org/10.1002/zaac.202100182>

strength. It has been shown that the chemical activity, electronic and optical properties of carbon materials can be tuned by adding suitable functional groups.^[27] Graphene oxide (GO) contains a monoatomic layer of functionalized (oxidized) graphene and has been used as an electrode modification material due to its special performance.^[28] GO has a high specific surface area, excellent electrochemical properties, and can be chemically coupled with nanoparticles,^[29] organic compounds,^[30] and biomolecules.^[31]

Currently, ion-imprinted polymers (IIPs)^[32] are widely used for the detection of trace metal ions due to its stability^[33] low cost^[34] and ease of preparation.^[35] Usually, we synthesize IIPs by mixing functional monomers, target ions (templates)^[36] and excess cross-linking agent. After polymerization, the template ions are eluted from the polymer to form a binding point^[37] that is completely complementary to the size, shape and function of the measured element, which is beneficial to the combination with the target element.^[38] At present, this technology is combined with various methods such as spectrophotometry and electrochemistry, and has been successfully used for trace detection of metal ions such as chromium,^[39] copper,^[40] silver,^[41] lead,^[42] and cadmium.^[43] Since the cavity of the imprinted polymer can coordinate with related metal ions, and the coordination between the metal and the ligand is relatively stable to the non-covalent bond, at the same time, the binding and breaking speed of the coordination bond can be controlled by changing the environmental conditions,^[44] so the method has excellent selectivity and stability. Even under harsh chemical conditions, IIPs have excellent stability and durability. At present, IIPs modified electrodes based on electrochemical detection have also been successfully applied to a variety of metal ions.^[45]

In this paper, we report a carbon paste electrode electrochemical sensor based on ion-imprinted sol-gel modification. For the first time, a carbon paste electrode modified with a bipolar tetradentate macrocyclic ligand H₄L ion imprinted polymer was prepared for the highly sensitive and selective detection of UO₂²⁺. The U-IIP and blank control non-imprinted polymer (N-IIP) were synthesized separately. In addition, the design, synthesis, characterization and combination with UO₂²⁺ of these ion-imprinted sol-gel materials are also introduced in detail. The introduction of GO has also enhanced the sensor's response to template ions. The constructed electrochemical sensor is cheap, stable, sensitive and has rapid response. It has been successfully applied to the analysis of water samples of Xiangjiang river and soil samples around uranium tailings.

Experimental Section

Instruments and reagents

All electrochemical tests were completed by CHI-660 C electrochemical workstation (Shanghai Chenhua Instrument Co., Ltd.). The standard three-electrode system includes: U-IIP/GO/CPE as the working electrode, saturated calomel electrode (SCE) as the reference electrode and platinum electrode as the counter electrode. Energy dispersive spectroscopy (EDS) analysis was performed on JSM-6700F scanning electron microscope (SEM), and the other equipment includes: Bruker 400-MHz nuclear magnetic

resonance spectrometer (Brooker), pHs-10 C digital acidity meter (Shanghai Lei Magnetic Scientific Instrument Factory). All the chemicals involved in the experiment were analytically pure. N,N-dimethylformamide (DMF), 3-aminopropyltrimethoxysilane (APTMS), GO, tetraethoxysilane (TEOS), phosphorus oxychloride (POCl₃), benzaldehyde, pyrrole, ortho-phenylenediamine and trifluoroacetic acid (TFA) were purchased from Aladdin Reagents Co., Ltd (Shanghai, P.R. China). Uranyl nitrate hexahydrate was purchased from Hubei Chushengwei Chemical Co., Ltd (Wuhan, P.R. China). Redistilled water was used throughout the experiment, and all solutions were prepared according to the conventional method.

Synthesis of H₄L

According to the preparation method of reference,^[46] we optimized and successfully synthesized H₄L. For the specific steps, please refer to the supporting information.

Preparation of carbon paste electrode modified by GO

First, pure graphite powder (4 g) and paraffin oil (1 mL) were added into a 25 mL beaker, and ethanol was used as the solvent. The mixture was stirred with a glass rod until a uniform paste was formed, and ultrasonic treatment lasted for 20 min. The mixture was then dried in an oven at 60 °C for 6 h to remove the solvent. Blocks of graphite were ground into powder using glass rods, and the powder was filled into a polyethylene plastic tube with a diameter of 3.5 mm and a length of 5 cm. Pressure was applied to the tube and the electrode was polished to achieve a smooth electrode surface. The other end was connected with a pencil lead. Finally, GO (5 mg) was dissolved in DMF (5 mL) and treated with ultrasound for 90 min. Drops of 30 μL of the above solution were added to the surface of the carbon paste electrode and the solvent was dried and evaporated at 35 °C. Thus the GO modified carbon paste electrode (GO/CPE) was fabricated.

Synthesis of U-IIP/GO/CPE and N-IIP/GO/CPE

We took H₄L (functional monomer) (1 mL, 1 mM) and UO₂²⁺ (template ion) (1.5 mL, 1 mM) and mixed them with ethanol at 35 °C for 30 min. Then, APTMS (stabilizer) (500 μL), TEOS (cross-linker) (100 μL) and NaOH (100 μL 1 M) were added and stirred at room temperature for 1.5 h to prepare a gel solution containing uranium ion template (U-IIP). The gel solution (N-IIP) as a blank control was prepared by replacing UO₂²⁺ (template ion) with 1.5 mL redistilled water. Finally, GO/CPE was immersed in the prepared U-IIP and N-IIP, respectively, so that the surface of the electrode was completely covered by the solution. Then, the electrode was placed at room temperature to evaporate and dry, so that midU-IIP/GO/CPE containing template ions and the blank control electrode N-IIP/GO/CPE were obtained. After that, 1.0 M HCl was prepared in a large beaker, and the beaker was placed in a dry magnetic stirrer. After adding magnets, stir the HCl slightly to make the surface of the HCl solution flow slowly, and the electrode surface was immersed in it to elute about 15 min. When the surface of the electrode changed from yellow to white, it indicated that the template ions on the midU-IIP/GO/CPE had been eluted, thereby U-IIP/GO/CPE was prepared. Then connected U-IIP/GO/CPE and N-IIP/GO/CPE to the electrochemical workstation for comparison experiments (Figure 1A). The combination of UO₂²⁺ and H₄L is shown in Figure 1B.

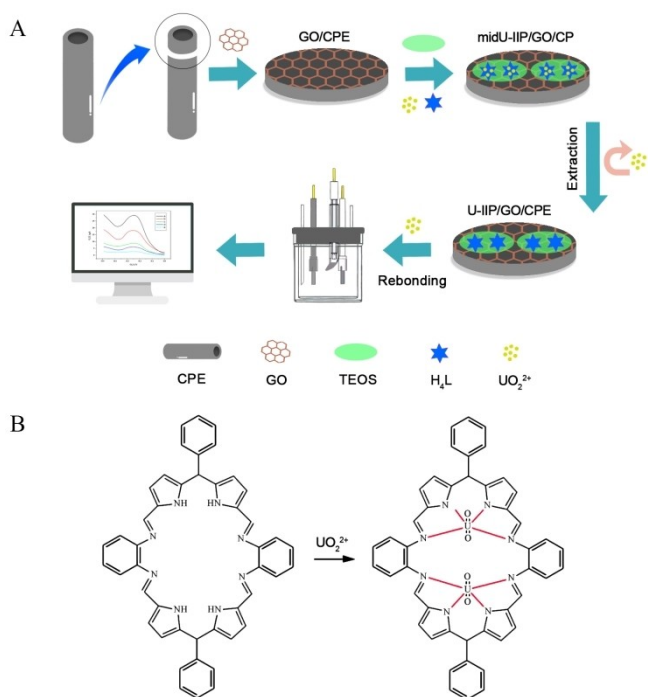


Figure 1. (A) Preparation schematic diagram of U-IIP/GO/CPE; (B) Combination of UO₂²⁺ and H₄L.

Electrochemical determination

An electrochemical workstation was connected to construct a standard three-electrode system: platinum as the counter electrode, saturated glycerin as the reference electrode, and U-IIP/GO/CPE as the working electrode. First, U-IIP/GO/CPE was put into 5 ml UO₂²⁺ solution for testing, and the open-circuit adsorption was conducted for 20 min. The electrode was then immersed in a buffer solution containing KCl (0.1 M) and Tris-HCl (0.1 M, pH=7.3) for the DPV test. The potential scanning range was -0.5 V to 0 V, the potential increment was 20 mV, the scanning rate was 120 mVs⁻¹, the pulse width was 120 ms, and the pulse amplitude was 50 mV.

2. Results and Discussion

2.1. Study of the spectral properties of H₄L

The spectral properties of H₄L are shown in supporting information.

2.2. Characterization of sensors

The GO/CPE, midU-IIP/GO/CPE, N-IIP/GO/CPE and U-IIP/GO/CPE were scanned by scanning electron microscope (SEM) to investigate their nanoscale surface properties and characteristics. As expected, the surface of GO/CPE (Figure 2A) has many scattered filamentous stripes, indicating that GO can be well absorbed and dispersed on the bare carbon paste electrode. In addition, the surface of N-IIP/GO/CPE (Figure 2B) is tighter than

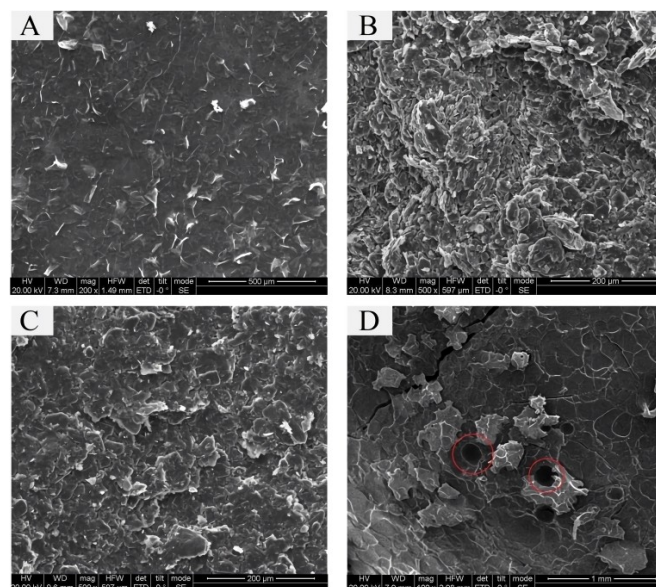


Figure 2. SEM images the surface of electrodes (A) GO/CPE; (B) N-IIP/GO/CPE; (C) midU-IIP/GO/CPE; (D) U-IIP/GO/CPE.

that of midU-IIP/GO/CPE (Figure 2C), because the surface of N-IIP/GO/CPE does not form an imprinting cavity, while the surface of midU-IIP/GO/CPE is flatter, because the high concentration of UO₂²⁺ solution combines with the surface to form a gel-like film. However, the surface of the electrode after elution (U-IIP/GO/CPE) is relatively rough, which just indicates the successful formation of ion imprinting binding sites and cavities on the electrode surface (Figure 2D)

2.3. Electrochemical characterization of U-IIP/GO/CPE sensor

2.3.1. Template elution and rebinding experiment

DPV was used to explore the elution and recombination of templates on different sensors under the same conditions. The peak current of midU-IIP/GO/CPE occurs at -0.26 V (Figure 3Ab), while the peak current is very weak after removal of template ions by HCl (1 M) elution, indicating that template ions have been effectively removed (Figure 3Ae). After immersing U-IIP/GO/CPE in UO₂²⁺ solution (2.8 μM) for 20 min, it can be seen from Figure 3Aa that the detected peak current is significantly higher than that of the N-IIP/GO/CPE (Figure 3Ac) control group, which is about 3 times the peak current detected in GO/CPE (Figure 3Ad). The reason may be that N-IIP/GO/CPE does not contain an ion-imprinted cavity, and UO₂²⁺ cannot undergo redox reactions on the electrode surface, resulting in a weak voltammetric signal. Therefore, it can be concluded that the ion imprinted cavities on U-IIP/GO/CPE greatly enhance the coordination with UO₂²⁺ and improve the sensor sensitivity.

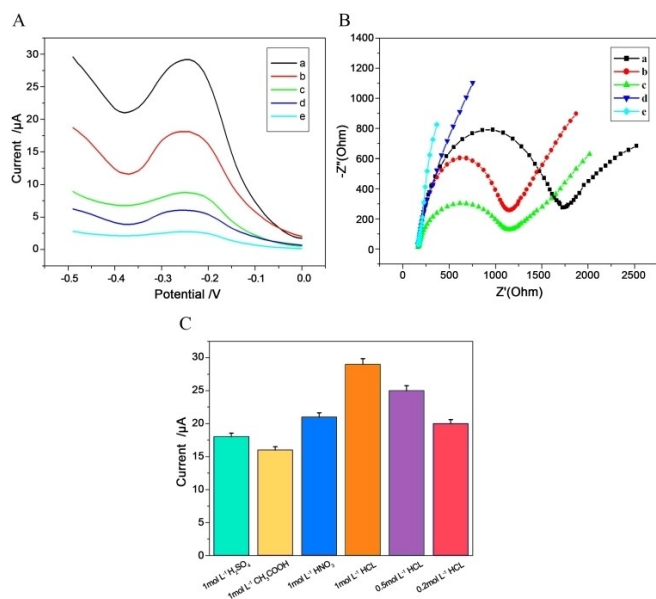


Figure 3. (A) Schematic diagram of response current DPV: (a) Detect $2.8 \mu\text{M UO}_2^{2+}$ with U-IIP/GO/CPE; (b) Detect $2.8 \mu\text{M UO}_2^{2+}$ with midU-IIP/GO/CPE; (c) Detect $2.8 \mu\text{M UO}_2^{2+}$ with N-IIP/GO/CPE; (d) Detect $2.8 \mu\text{M UO}_2^{2+}$ with GO/CPE; (e) DPV Signals of U-IIP/GO/CPE in buffer solution; (B) Impedance spectrum at $2 \text{ mM K}_3\text{Fe}(\text{CN})_6/\text{K}_4\text{Fe}(\text{CN})_6$: (a) N-IIP/GO/CPE; (b) GO/CPE; (c) midU-IIP/GO/CPE; (d) U-IIP/GO/CPE (added $2.8 \mu\text{M UO}_2^{2+}$); (e) U-IIP/GO/CPE; (C) Effect of inorganic acid eluent on the detection of uranyl ions by U-IIP/GO/CPE.

2.3.2. Electrochemical impedance diagram

Electrochemical Impedance Spectroscopy (EIS) was used to analyze the electrochemical properties of different sensor surfaces. The mixed solution of $\text{K}_3\text{Fe}(\text{CN})_6/\text{K}_4\text{Fe}(\text{CN})_6$ (2.0 mM) and potassium chloride (0.2 M) was used for electrochemical study at a frequency ranging from 0.1 Hz to 100000 Hz , signal amplitude of 5 mV and potential of 0.25 V . ZView software was used to fit the electrochemical impedance data, and the resistance values (R_{ct}) of different sensors were obtained (Figure 3B). It can be seen from the figure that the GO/CPE impedance is 1987Ω (Figure 3Bb), and when the GO/CPE is covered with the ion-imprinted polymer, R_{ct} drops to 1625Ω (Figure 3Bc), indicating that the polymer layer has been successfully constructed, and the ion-imprinted polymer layer can accelerate charge transfer. The impedance value of N-IIP/GO/CPE is 2512Ω (Figure 3Ba), which is much larger than the R_{ct} of midU-IIP/GO/CPE (Figure 3Bc), mainly due to the lack of probe channels on the N-IIP/GO/CPE surface. However, the R_{ct} of U-IIP/GO/CPE decreases to 389Ω (Figure 3Be), indicating that the probe channel has been successfully constructed and imprinted holes formed on the surface of the sensor, thus promoting the passage of probe molecules. It can be seen from Figure 3Bd that when the U-IIP/GO/CPE is immersed in $2.8 \mu\text{M UO}_2^{2+}$ solution for 20 min , the R_{ct} value of the sensor increases to 876Ω , which indicates that the imprinting holes are

occupied after the sensor is combined with UO_2^{2+} , resulting in an increase in the R_{ct} value.

2.4. Optimization of experimental conditions

2.4.1. Optimization of sol-gel conditions

In the whole process of preparing gel, the ligand H_4L complexed with uranyl ions to form the complex. The amount of APTMS, TEOS, NaOH added and the reaction time of forming sol-gel film are very important in the experimental process. The single variable method was used in the experiment. When the amount of cross-linking agent (TEOS) was too small, the template ion could not be cross-linked with the polymer well, which affected the determination of the experiment. When TEOS was excessive, it was difficult for the template ions to elute from the imprinted cavity, which affected the elution-recombination experiment. Finally, we found that the optimal reaction conditions were APTMS ($500 \mu\text{L}$), TEOS ($300 \mu\text{L}$), NaOH ($50 \mu\text{L}$, 1 M), and the reaction time was 1.5 h .

2.4.2. Optimization of the eluent and elution time

The elution of template ions from midU-IIP/GO/CPE is a key step for subsequent ion recombination and electrochemical detection. The eluted electrode has a stronger electrical signal in the detection solution. The experiment used sulfuric acid, acetic acid, nitric acid and hydrochloric acid at different concentrations to select the best eluent for the elution rate of UO_2^{2+} . It can be seen from Figure 3C that the elution efficiency of 1 M HCl is the highest, and a strong electrical signal is displayed on the electrode surface. At the same concentration, the elution rate of hydrochloric acid is higher than that of other inorganic acids, which may be attributed to the increase of heteroatoms in the ligands by protonation. In addition, the influence of time on the elution effect was studied, and HCl (1 M) was used as the eluent. We found that 15 min is the best time for elution efficiency.

2.4.3. Effect of pH

After exploring the influence of HAc-NaAc, citric acid-sodium citrate, Tris-HCl, phosphoric acid-sodium phosphate and other buffer solutions on the current intensity of the sensor, Tris-HCl was finally selected as the best buffer solution. In addition, the pH of the buffer solution is also very important for the detection current of the sensor. We detected the influence of the pH value on the sensor in the range of 4.0 to 9.0 , and the results are shown in Figure 4A. The data shows that the electrode response drops sharply when the pH value is lower than 7.3 . This is due to the protonation of the nitrogen atom of the H_4L functional group on U-IIP/GO/CPE, which weakens the interaction between UO_2^{2+} and the electron pair on the nitrogen atom of the H_4L functional group. On the other hand, at a pH higher than 7.3 , metal ions may be hydrolyzed, and the formation of negatively charged salts and

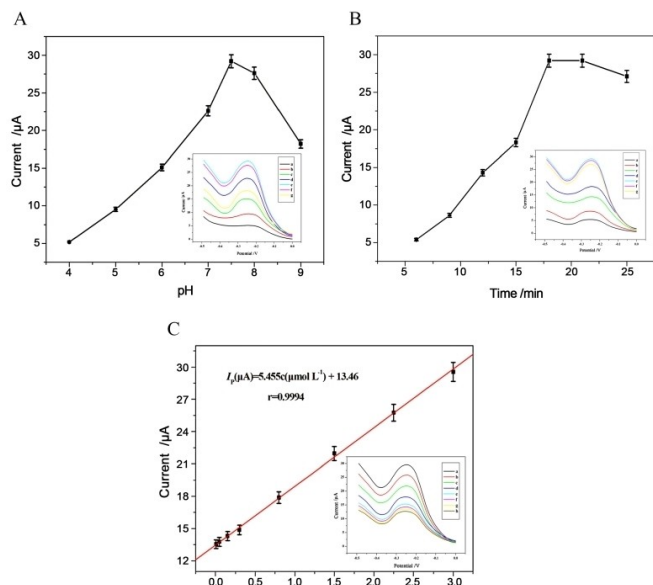


Figure 4. (A) Effect of pH on the sensor when detecting uranyl ions; (B) Effect of enrichment time on detection of UO_2^{2+} by U-IIP/GO/CPE; (C) Current and calibration curve of U-IIP/GO/CPE at different concentrations of uranyl ions (concentrations from top to bottom: 3.0, 2.25, 1.5, 0.8, 0.3, 0.15, 0.05, 0.01 μM).

hydroxyl complexes may prevent the interaction of UO_2^{2+} with H_4L in the sol-gel polymer. As a result, the volt-ampere response is reduced. Therefore, the Tris-HCl buffer solution with $pH = 7.3$ was selected as the best condition for this experiment.

2.4.4. Optimization of enrichment time

Under optimal experimental conditions, the other experimental conditions were kept unchanged, and the influence of the enrichment time on the sensitivity of the sensor in the 5~25 min period was studied. The results are shown in Figure 4B. It can be seen that before 20 min, with the increase of the enrichment time, the voltammetric signal intensity increases significantly, until the adsorption equilibrium is reached at 20 min. This phenomenon can be attributed to the adsorption saturation of the electrode surface. However, with the further increase of the enrichment time, the voltammetry signal weakly attenuate. Thus, 20 min was chosen as the best adsorption time in this experiment.

2.5. Performance of U-IIP/GO/CPE sensors

2.5.1. U-IIP/GO/CPE sensor calibration curves and detection limits

Under the optimal experimental conditions, the U-IIP/GO/CPE sensor system was placed in different concentrations of UO_2^{2+} solution, and the DPV detection data was used to draw Figure 4C. It can be seen from the figure that the peak current is proportional to the concentration of UO_2^{2+} in the range of

0.01 μM to 3.0 μM . The fitted linear equation is $I_p(\mu A) = 5.455c(\mu mol L^{-1}) + 13.46$, and the correlation coefficient $R = 0.998$. On this basis, according to the formula $S/N = 3$ and $S/N = 10$, the method detection limit (MDL) and the limit of quantification (LOQ)^[47] can be obtained respectively. Therefore, the MDL and LOQ of the method based on this range are about 1.32 nM and 4.4 nM. Where "S" is the standard deviation of the intercept and "N" is the slope.

2.5.2. Experimental study of interference and selectivity of ion imprinting sensors

In order to test the specificity of the sensor for UO_2^{2+} recognition, after adding 2.8 μM UO_2^{2+} to the detection solution, a solution containing 10 times the concentration of Co^{2+} , Zn^{2+} , Cu^{2+} , Ni^{2+} and other metal ions was added. The experimental results show that when Fe^{2+} , Cd^{2+} , Mn^{2+} , Fe^{3+} , Ag^+ , Co^{2+} , Cr^{3+} , Al^{3+} and Pb^{2+} are interfering cations, the voltammetric signal of the modified electrode is not affected, which indicates that the electrode has good selectivity for UO_2^{2+} . As shown in Figure 5Aa, when the Hg^{2+} / UO_2^{2+} concentration ratio is 10, the influence of Hg^{2+} on the DPV signal is also negligible; and when the concentration ratio is greater than 10, Hg^{2+} will partially affect the electrode signal (Figure 5Ab), but the masking agent can be added to reduce interference. In addition, Figure 5B shows that N-IIP/GO/CPE has no obvious response signal to UO_2^{2+} at -0.26 V, and the interference is very obvious when only Hg^{2+} is present in the solution. Therefore, comparing the two figures shows that the U-IIP/GO/CPE sensor has a good recognition performance for UO_2^{2+} .

2.5.3. Stability and reproducibility of U-IIP/GO/CPE

The experiment also studied the repeatability and stability of the U-IIP/GO/CPE sensing system. Using the same experimental conditions on the same modified electrode, the concentration of 2.8 μM UO_2^{2+} solution was determined 6 times, and the relative standard deviation (RSD) was 4.60%. The repeatability of the electrode was evaluated with five different electrodes (built using the same procedure), and the RSD was 3.90%. In

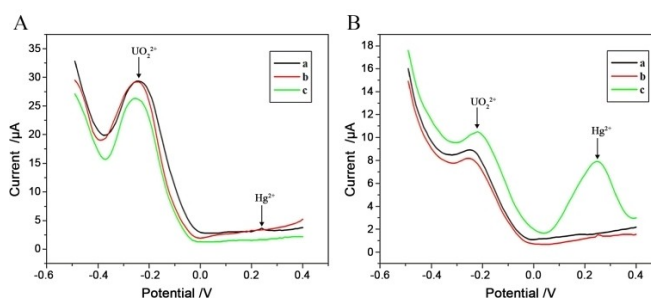


Figure 5. (A) The response of U-IIP/GO/CPE in 2.8 μM UO_2^{2+} and Hg^{2+} : (a) 2.8 μM UO_2^{2+} and Hg^{2+} ; (b) 2.8 μM UO_2^{2+} and 28 μM Hg^{2+} ; (c) 2.8 μM Hg^{2+} in 0.1 M KCl and Tris-HCl buffer at $pH = 7.3$; (B) the same experiment with N-IIP/GO/CPE.

Table 1. U-IIP/GO/CPE sensors for UO_2^{2+} analysis in actual samples ($n=6$).

Sample	This method Added UO_2^{2+} (μM)	Found (μM)	Relative recovery (%)	RSD (%)	ICP-MS Found (μM)	Relative recovery (%)	RSD (%)	t-test ^[a]
Soil sample 1	0.25	0.239	95.45	2.51	0.240	95.83	1.52	0.352
Soil sample 2	0.25	0.266	106.25	3.25	0.257	102.86	2.36	1.967
Soil sample 3	0.25	0.241	96.55	2.92	0.245	97.91	1.95	0.960
Water sample 1	0.50	0.486	97.22	3.05	0.483	96.55	1.21	0.515
Water sample 2	0.50	0.511	102.22	2.23	0.519	103.85	2.20	1.273

^[a] Tabulated t-value for four degrees of freedom at 95% confidence level is 2.228.

addition, after one month of storage under dry conditions at room temperature, the long-term stability of the prepared sensor was tested. For the same uranyl ion solution, the current response value reached 95% of the original response value, which indicates that the modified electrode has good stability.

2.5.4. Test the performance of real samples

In order to test the performance of the sensor in real samples, we collected soil samples from uranium tailings around Hengyang City and water samples from the Xiangjiang River for analysis. The soil sample was prepared into a solution using a specific method (see supporting information), and the samples were added to the test container to be tested according to the above-mentioned best experimental method. Each sample was added, detected, and recovered using the standard addition method, and six parallel determinations were performed on each sample. UO_2^{2+} solutions with a concentration of 0.25 μM and 0.50 μM were added to the soil and water samples to be tested respectively. The experimental data in Table 1 shows that the sample recovery rate is between 95.45% and 106.25%, and the relative standard deviation is 2.23% to 3.25%. In addition, the method was compared with the inductively coupled plasma mass spectrometry (ICP-MS) method, and the results were within 95% confidence level and acceptable error range. At the same time, we used the standard addition method to perform repeated experiments on three sets of samples, and analyzed the precision of the method. The intra-day precision (6 parallel experiments were performed in each group in one day) was 4.60% or less, and the inter-day precision (the electrode was placed for about a month and the experiments were carried out on 3 different days, each group performs 6 parallel experiments) was 5.16% or less. The t-test was used to evaluate

the statistical difference between this method and ICP-MS, and the results show that the detection precision of the two methods is not significantly different. This shows that the prepared U-IIP/GO/CPE is suitable for the determination of trace uranium ions in real samples and has good stability.

2.6. Comparison of the sensor reported in this article with other electrochemical sensors in the literatures for UO_2^{2+}

Comparing this work with other electrochemical sensors, it can be seen intuitively from Table 2 that the U-IIP/GO/CPE electrochemical sensor has a wider linear relationship and a lower detection limit. Moreover, the electrode is easy to prepare and low in cost, and each modified electrode is about 0.8 dollars. Therefore, this sensor has potential value for the detection of trace UO_2^{2+} .

3. Conclusions

In this work, a new type of electrochemical sensor for the determination of trace uranyl ions was prepared for the first time in a carbon paste electrode modified by ion imprinting combined with bipolar tetradentate functional monomer H_4L . Compared with U-IIP/GO/CPE and N-IIP/GO/CPE, the electrode modified with ion imprinting made the sensor's specific recognition of uranium ions enhanced significantly. In addition, the addition of GO increased the specific surface area of the sensor and optimized the conductivity of the electrode, thereby obtaining an ideal electrochemical response. It also had excellent selectivity in the presence of high concentrations of interfering ions. At the same time, the use of ICP-MS technology as a comparative verification for the detection of uranium concentration indicates that this electrochemical sensing

Table 2. Comparison of electrochemical sensor performance between U-IIP/GO/CPE and other literatures.

Electrode	Method	Linear range (μM)	Detection limit (μM)	References
$\text{Pt}_1\text{Ru}_2\text{-PCs/GCE}$	DPV	0.168–3.528	0.024	[18]
MMIP/MCPE	DPV	0.06–50	0.0173	[44]
Au/NPCs-GCE	DPV	0.12–95.1	0.0494	[48]
GRA-SPEs	DPV	0.005–0.1	0.0045	[49]
U-IIP/GO/CPE	DPV	0.01–3.0	0.00132	This work

system has the advantages of sensitivity, high precision, good reproducibility, low method detection limit, and system stability. Moreover, the cost of each modified electrode is very low, which is conducive to further promotion as a probe for detecting UO_2^{2+} . Therefore, the U-IIP/GO/CPE sensing system may be able to provide a reference for the further preparation of electrochemical sensors for the detection of uranyl ions.

Acknowledgements

This work was financially supported by the National Natural Science Foundation of China (11475079), the Natural Science Foundation of Hunan Province (No. 2019JJ40244), Hengyang science and technology planning project (No. 202010031546) and Open Fund Project of State Key Laboratory of Chemo-Biosensing and Metrology (Hunan University) (2018014). The authors declare that they have no competing interests.

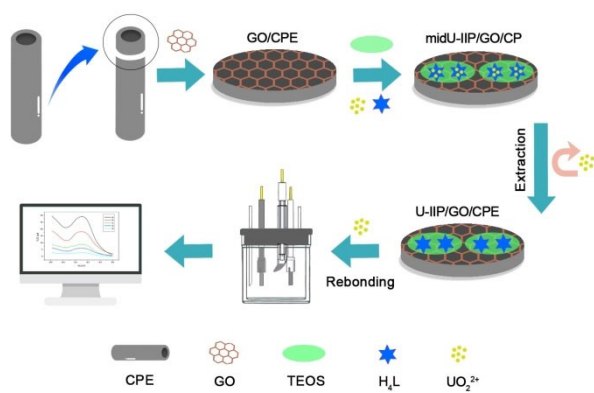
Keywords: Electrochemistry · Trace analysis · Uranyl ions · Ion-imprinting · Graphene oxide

- [1] T. Kim, T. H. Tran, S. Y. Hwang, J. Park, D. X. Oh, B.-S. Kim, *ACS Nano* **2019**, *13*, 3796–3805.
- [2] K. Vohra, A. Vodonos, J. Schwartz, E. A. Marais, M. P. Sulprizio, L. J. Mickley, *Environ. Res.* **2021**, *195*, 110754.
- [3] S. A. Sarkodie, S. Adams, *Sci. Total Environ.* **2018**, *643*, 1590–1601.
- [4] D. Dewar, in *Nuclear Non-Proliferation in International Law-Volume IV*, Springer, **2019**, pp. 229–235.
- [5] S. Wang, Y. Ran, B. Lu, J. Li, H. Kuang, L. Gong, Y. Hao, *Biol. Trace Elem. Res.* **2019**, 1–10.
- [6] H. Takahashi, Y. Izumoto, T. Matsuyama, H. Yoshii, *X-Ray Spectrom.* **2019**, *48*, 366–374.
- [7] Z. Gao, W. Zhong, *Anal. Bioanal. Chem.* **2021**, 1–16.
- [8] H. Ahmad, U. Haseen, K. Umar, M. S. Ansari, M. N. M. Ibrahim, *Microchim. Acta* **2019**, *186*, 649.
- [9] S. Wang, H. Chen, B. Sun, *Food Chem.* **2020**, *315*, 126158.
- [10] S. V. Jovanovic, T. Kell, J. El-Haddad, C. Cochrane, C. Drummond, A. El-Jaby, *J. Radioanal. Nucl. Chem.* **2020**, *323*, 831–838.
- [11] M. Schneider, H. R. Cadorim, B. Welz, E. Carasek, J. Feldmann, *Talanta* **2018**, *188*, 722–728.
- [12] K. Danhana, C. T. de Souza, E. Palacio, V. Cerdà, *Microchem. J.* **2019**, *150*, 104148.
- [13] S. Zheng, H. Wang, Q. Hu, Y. Wang, J. Hu, F. Zhou, P. Liu, *Sens. Actuators B* **2017**, *253*, 766–772.
- [14] B. Ozden, C. Brennan, S. Landsberger, *Environmental Earth Sciences* **2019**, *78*, 114.
- [15] B. Zheng, J. Li, Z. Zheng, C. Zhang, C. Huang, J. Hong, Y. Li, J. Wang, *Opt. Laser Technol.* **2021**, *133*, 106522.
- [16] T. Liu, J. Yuan, B. Zhang, W. Liu, L. Lin, Y. Meng, S. Yin, C. Liu, F. Luan, *Environ. Sci. Technol.* **2019**, *53*, 14612–14619.
- [17] Z. Zhou, Y. Zhou, X. Liang, F. Xie, S. Liu, J. Ma, *J. Radioanal. Nucl. Chem.* **2019**, *322*, 2049–2056.
- [18] X. Cao, Y. Sun, Y. Wang, Z. Zhang, Y. Dai, Y. Liu, Y. Wang, Y. Liu, *J. Solid State Electrochem.* **2021**, *25*, 425–433.
- [19] I. Geça, M. Ochab, M. Korolczuk, *Talanta* **2020**, *207*, 120309.
- [20] S. Güney, O. Güney, *Sens. Actuators B* **2016**, *231*, 45–53.
- [21] L. A. Romero-Cano, A. I. Zárate-Guzmán, F. Carrasco-Marín, L. V. González-Gutiérrez, *J. Electroanal. Chem.* **2019**, *837*, 22–29.
- [22] U. Pinaeva, T. C. Dietz, M. Al Sheikhly, E. Balanzat, M. Castellino, T. L. Wade, M. C. Clochard, *Reactive and Functional Polymers* **2019**, *142*, 77–86.
- [23] X. Wu, Q. Huang, Y. Mao, X. Wang, Y. Wang, Q. Hu, H. Wang, X. Wang, *TrAC Trends Anal. Chem.* **2019**, *118*, 89–111.
- [24] Z. F. Akl, T. A. Ali, *J. Radioanal. Nucl. Chem.* **2017**, *314*, 1865–1875.
- [25] Y. Liao, M. Wang, D. Chen, *Appl. Surf. Sci.* **2019**, *484*, 83–96.
- [26] A. Özcan, M. Gürbüz, A. A. Özcan, *Talanta* **2018**, *187*, 125–132.
- [27] H. Lee, T. K. Choi, Y. B. Lee, H. R. Cho, R. Ghaffari, L. Wang, H. J. Choi, T. D. Chung, N. Lu, T. Hyeon, *Nat. Nanotechnol.* **2016**, *11*, 566–572.
- [28] P. Reanpang, J. Upan, J. Jakmunee, *Talanta* **2021**, 122493.
- [29] Z. Zhang, F. Ahmad, W. Zhao, W. Yan, W. Zhang, H. Huang, C. Ma, J. Zeng, *Nano Lett.* **2019**, *19*, 4029–4034.
- [30] H. Yan, Y. Xie, Y. Jiao, A. Wu, C. Tian, X. Zhang, L. Wang, H. Fu, *Adv. Mater.* **2018**, *30*, 1704156.
- [31] P. Chen, K. Xu, T. Zhou, Y. Tong, J. Wu, H. Cheng, X. Lu, H. Ding, C. Wu, Y. Xie, *Angew. Chem. Int. Ed.* **2016**, *55*, 2488–2492; *Angew. Chem.* **2016**, *128*, 2534–2538.
- [32] C. Lin, H. Wang, Y. Wang, L. Zhou, J. Liang, *Int. J. Environ. Anal. Chem.* **2011**, *91*, 1050–1061.
- [33] M. M. Yusoff, N. R. N. Mostapa, M. S. Sarkar, T. K. Biswas, M. L. Rahman, S. E. Arshad, M. S. Sarjadi, A. D. Kulkarni, *Journal of Rare Earths* **2017**, *35*, 177–186.
- [34] J. Muñoz, R. Montes, J. Bastos-Arrieta, M. Guardingo, F. Busqué, D. Ruiz-Molina, C. Palet, J. García-Orellana, M. Baeza, *Sens. Actuators B* **2018**, *273*, 1807–1815.
- [35] M. Yolcu, N. Dere, *Electroanalysis* **2018**, *30*, 1147–1154.
- [36] P. Yáñez-Sedeño, S. Campuzano, J. M. Pingarrón, *Anal. Chim. Acta* **2017**, *960*, 1–17.
- [37] F. An, B. Gao, X. Feng, *J. Appl. Polym. Sci.* **2009**, *112*, 2241–2246.
- [38] P. Peng, L. Liao, Z. Yu, M. Jiang, J. Deng, X. Xiao, *Int. J. Environ. Anal. Chem.* **2019**, *99*, 1495–1514.
- [39] S. Parvizi, M. Behbahani, A. Esrafil, *New J. Chem.* **2018**, *42*, 10357–10365.
- [40] S. Di Masi, A. Pennetta, A. Guerreiro, F. Canfarotta, G. E. De Benedetto, C. Malitesta, *Sens. Actuators B* **2020**, *307*, 127648.
- [41] M. Behbahani, F. Omid, M. G. Kakavandi, G. Hesam, *Appl. Organomet. Chem.* **2017**, *31*, e3758.
- [42] H. Ebrahimzadeh, M. Behbahani, *Arab. J. Chem.* **2017**, *10*, S2499–S2508.
- [43] V. Zarezade, M. Behbahani, F. Omid, H. S. Abandansari, G. Hesam, *RSC Adv.* **2016**, *6*, 103499–103507.
- [44] C. Su, Z. Li, D. Zhang, Z. Wang, X. Zhou, L. Liao, X. Xiao, *Biosens. Bioelectron.* **2020**, *148*, 111819.
- [45] H. Wang, D. Qian, X. Xiao, S. Gao, J. Cheng, B. He, L. Liao, J. Deng, *Biosens. Bioelectron.* **2017**, *94*, 663–670.
- [46] J. Wang, J. Xue, X. Xiao, L. Xu, M. Jiang, P. Peng, L. Liao, *Spectrochim. Acta Part A* **2017**, *187*, 104–109.
- [47] W. Zhang, Y. Hua, Q. Lu, W. Qiu, Y. Li, *Journal of Hygiene Research* **2021**, *50*, 625–632.
- [48] F. Li, R. Li, Y. Feng, T. Gong, M. Zhang, L. Wang, T. Meng, H. Jia, H. Wang, Y. Zhang, *Mater. Sci. Eng. C* **2019**, *95*, 78–85.
- [49] V. T. Kostaki, A. B. Florou, M. I. Prodromidis, *Electrochim. Acta* **2011**, *56*, 8857–8860.

Manuscript received: May 23, 2021

Revised manuscript received: August 10, 2021

Accepted manuscript online: August 20, 2021



Y. Li, Z. Wang, C. Liu, D. Zhang,
Prof. L. Liao, Prof. Dr. X. Xiao*

1 – 8

Graphene oxide modified H₄L-ion
imprinting electrochemical sensor
for the detection of uranyl ions

